

Nonlinear analysis of service stresses in reinforced concrete sections-closed form solutions

Helena F.M. Barros*¹ and Rogério A.F. Martins²

¹Institute for Systems Engineering and Computers at Coimbra (INESC Coimbra),
Department of Civil Engineering, Faculty of Sciences and Technology University of Coimbra, Portugal

²Engineering Faculty, Lusíada University, V N Famalicão, Portugal

(Received May 20, 2010, Revised April 24, 2012, Accepted May 30, 2012)

Abstract. This paper presents an algorithm for the evaluation of stresses in reinforced concrete sections under service loads. The algorithm is applicable to any section defined by polygonal contours and is based on an analytical integration of the stresses. The nonlinear behaviour of concrete is represented by the parabola-rectangle law used in the Eurocode-2 for the ultimate concrete design. An integrated definition of the strains in concrete and steel is possible by the use of Heaviside functions, similarly to what is done for ultimate section design in Barros *et al.* (2004). Other constitutive equations for the definition of the stresses in the concrete or steel can be easily incorporated into the code. The examples presented consist in the evaluation of resulting axial load and bending moment in an irregular section and in a section in L shape. The results, for service stresses, can also be plotted in terms of design abacus; a rectangular doubly reinforced section is presented as example.

Keywords: reinforced concrete; serviceability limit state; stress control; analytical solution; design abacus.

1. Introduction

The design of reinforced concrete structures considers two levels of loads, namely ultimate and service loads. Ultimate conditions correspond to the rupture of the section usually evaluated in terms of maximum bending moment and axial load. In general, that is, if are excluded the cases in which the stress-strain diagrams have descending branches, the rupture of a section under maximum loading can occur either by attaining ultimate strain in concrete or in steel. The authors (Barros *et al.* 2003, 2004), present a method that permits the use of unique expressions defining the concrete strain in the most stressed fibre of the section, as needed for ultimate design. The method is general and is independent of the stress-strain laws used to define concrete and steel stresses. In Eurocode-2 the concrete stress-strain relation used is the parabola-rectangle law, with different parameters that depend on the concrete strength. Other nonlinear expressions are indicated in MC90, namely for the nonlinear analysis of concrete structures under service limit states. A comparative analysis of the provisions in ACI 318-05 and Eurocode 2 (EC2-94) is made by Hawileh *et al.* (2009), identifying differences in these codes in what regards to flexural concrete design. Campion (2008) presents a model to predict the response of concrete columns under variable confinement stresses. In Papadakis (2007) an evaluation is made of the concrete service life using fundamental mathematical

* Corresponding author, Professor, E-mail: hbarros@dec.uc.pt

models that simulate the deterioration mechanisms, such as carbonation and chloride penetration. Lou *et al.* (2008) perform the integration the tangent stiffness by dividing the section into several concrete trapezoids. Sadjadi *et al.* (2010) implement a fiber element model into a computer program and a tri-linear stress-strain relationship for steel behaviour. Chaudhary *et al.* (2007) develop closed form expressions for stiffness matrix, load vector and mid-span deflection of beam elements under service loads. In Lam *et al.* (2009) formulas are developed for the direct evaluation of the maximum axial load level and minimum confining pressure in order to guarantee a nominal flexural ductility in high-strength concrete columns. Alnuaimi (2007) presents an experimental and analytical study of partially prestressed concrete beams under the combined effect of bending, shear and torsion loads. Design tables of concrete sections and a procedure to design reinforced concrete structures are proposed in Fragiadakis and Papadarakis (2008). A new generic fiber model algorithm is implemented by Charalampakis and Koumousis (2008), allowing the integration of stress within composite sections. In Pallares *et al.* (2009) is developed a numerical method to iterate a system of equations obtained in the design of reinforced concrete sections subjected to axial forces and biaxial bending. In Sousa *et al.* (2007) a procedure for the analytical integration of section resistant forces and tangent moduli in reinforced concrete frames is presented. Bonet *et al.* (2006) make a comparative analysis between numerical and analytical integration of concrete stresses for ultimate design. Ruiz *et al.* (2007) present a closed form solution of the bond stresses in reinforced concrete.

In the algorithm developed by Barros *et al.* (2006), the concrete section is divided into triangles with exact integration of stresses in each one. Since the section is defined by an arbitrary polygonal line, the model can be used in any type of section. The present paper is an improvement of this work, Barros *et al.* (2006), with the analysis of the section under increasing service stresses up to the ultimate state. The conditions of rupture of a reinforced concrete section are stated in terms of concrete or steel maximum strain with parametric equations. These conditions are solved in an unique equation by the use of Heaviside functions and implemented into the mathematical manipulation software MAPLE. The expressions of these equations for the force F and stress σ_s , are shown on appendix A. Similar but longer expressions are obtained for the moments M_x and M_y . To show the application of the model, several examples consisting of arbitrary shape, L and rectangular sections are presented. The integration procedure is used in the evaluation of interaction surfaces for the ultimate design of reinforced concrete columns, Barros *et al.* (2005).

An advantage of the work here presented consists of the possibility of making the exact integration of the stresses in the compressed concrete considering a section with any arbitrary shape. This is relevant since it can be applied to T-sections, L-sections and others. In the work of Silva *et al.* (2009) the integration procedure is applied to the ultimate design of reinforced concrete sections under axial load and biaxial bending moment. Another advantage is the fact that this algorithm allows, for service limit states, the consideration of any nonlinear constitutive law. In the present case the parabola-rectangle law as defined in the Eurocode 2 is adopted. The method is particularly attractive in dealing with service limit states, once that it is current in practice, for these situations, to use linear laws.

Examples are presented that show the applicability of the method in obtaining the exact solution to any desired degree of accuracy.

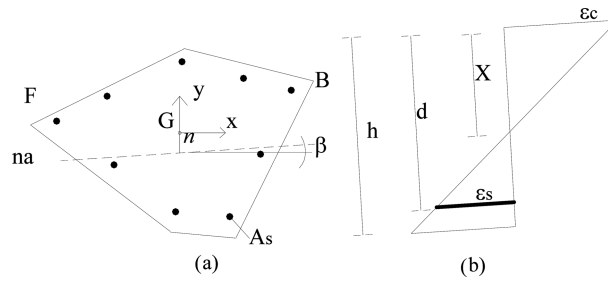


Fig. 1 (a) Geometry of the section and (b) Deformed section with strains in concrete ϵ_c and steel ϵ_s

2. Integration of compressive stresses in concrete

The reinforced concrete section to be studied in this work can be defined by an arbitrary polygonal line, as represented in Fig. 1(a). In this figure, G represents the centroid of the concrete section, the reference axis x and y being therefore baricentric. The neutral axis is represented by (na).

Denoting by β the angle of the neutral axis with the x axis and by n the ordinate at the origin, the neutral axis is defined by the following linear equation

$$y(x) = n + tg\beta x \tag{1}$$

Fig. 1(b) shows a lateral view of the section after deformation, satisfying a linear variation of strains. The strain in the most compressed concrete fibre, located at a distance X from the neutral axis, is denoted by ϵ_c . The strain in the opposite steel, at a distance d , is denoted by ϵ_s . The non dimensional parameter α is defined by

$$\alpha = \frac{X}{d} \tag{2}$$

2.1 Strain deformation of the section under ultimate conditions

To evaluate the rupture of the reinforced concrete section it is supposed that the deformation attains certain limits. Failure occurs whenever one of the following mechanisms is satisfied, (see Fig. 2):

- (1) Rupture by the steel when, at the most stressed fibre, the strain ϵ_s is equal to 1%, line 1

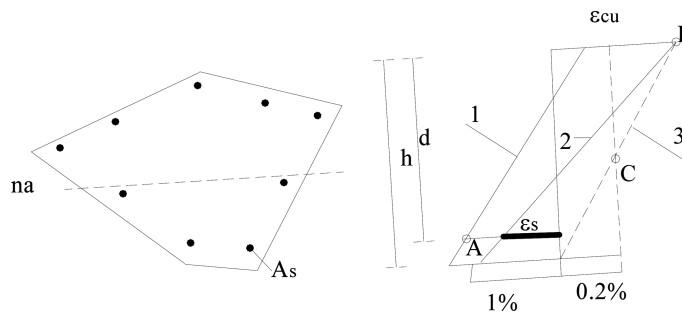


Fig. 2 Deformed section in rupture

(contains point A);

(2) Rupture by the concrete when the strain ϵ_c equals the ultimate value ϵ_{cu} , line 2 (contains point B);

(3) Rupture with the whole section under compression and the strain at point C equal to 0.2%, line 3 (contains point C).

The use of Heaviside functions, denoted by $H(\cdot)$, allows the definition of a sole equation for ϵ_c , as described by Barros *et al.* (2004), that is

$$\epsilon_c = \frac{1}{100} \frac{\alpha}{\alpha-1} - H\left(\alpha - \frac{\epsilon_{cu}}{\epsilon_{cu} + 1\%}\right) \left(\epsilon_{cu} + \frac{\alpha}{100(\alpha-1)}\right) + H(X-h) \left(\epsilon_{cu} - \frac{X}{X-3/7h} 0.2\%\right) \quad (3)$$

The strain ϵ_s at the most stressed steel fibre is obtained by the compatibility condition. It is given by the following function of the concrete strain ϵ_c

$$\epsilon_s = \epsilon_c \frac{d-X}{X} \quad (4)$$

and contains Heaviside functions as well.

2.2 Compressed concrete and stress integration

The neutral axis divides the section in two zones, one in compression, the other in tension. In order to integrate the stresses in the compressed concrete, the section is divided into triangles, as represented in Fig. 3. For simplicity the neutral axis in this figure is drawn outside the section, but it can lay anywhere.

The triangles, Fig. 3, are numbered starting by the one more distant to the neutral axis, as 1, 2 and 3. A general triangle is then considered denoting by A the more distant node and numbering the others in the direct sense such as AFB.

Let us consider a general triangle AFB, represented in Fig. 4. In order to perform the integration, this triangle is subdivided by drawing a line parallel to the neutral axis through B or F, into triangles T1 and T2.

Considering the triangle T1, any arbitrary point P within this triangle can be defined in area coordinates termed L_1, L_2 and L_3 , such that

$$L_1 = \frac{A_1}{A}; L_2 = \frac{A_2}{A}; L_3 = \frac{A_3}{A} \quad (5a,b,c)$$

where A is the area of triangle T1, and A_1, A_2 and A_3 are its subdivisions as indicated in Fig. 5. The

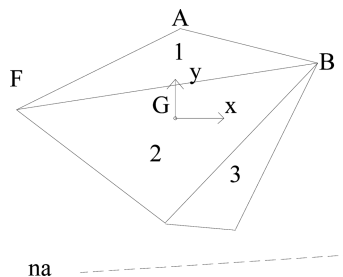


Fig. 3 Decomposition of the section into triangles

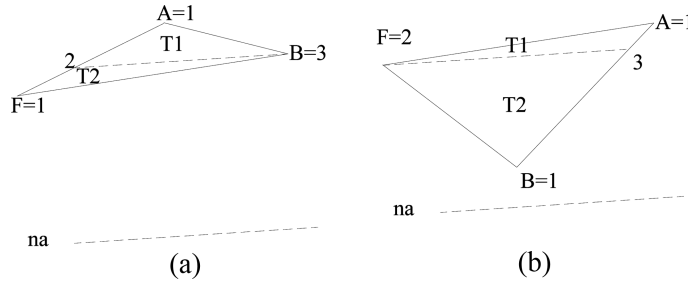


Fig. 4 (a) and (b) Decomposition of triangle AFB

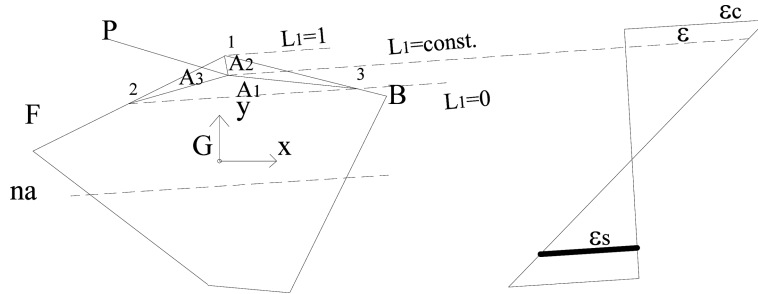


Fig. 5 Elementary triangle

deformation ε at this general point P is given by

$$\varepsilon = L_1(\varepsilon_1 - \varepsilon_2) + \varepsilon_2 \tag{6}$$

and is only function of coordinate L_1 . This is due to the fact that side 23 is parallel to the neutral axis and the strain is constant at all points located at the same distance to this axis. In this equation ε_1 represents the strain at point 1; ε_2 represents the strain at points 2 or 3, since they are the same.

In this formulation the stress $\sigma(\varepsilon)$ is also a function of L_1

$$\sigma = \sigma(L_1) \tag{7}$$

The resulting force F in the triangle 123 is obtained by the following integration

$$F = \int_{Area} \sigma(L_1) darea \tag{8}$$

Performing this integration it is found that

$$F = \int_0^1 \sigma(L_1)(1-L_1) \det J dL_1 \tag{9}$$

where $\det J$ represents the Jacobian of the transformation, equal to 2Δ , where Δ is the area of triangle 123. The formula for F is presented in Appendix A.

The bending moment over the side 23, termed M_{23} in Fig. 6, is given by

$$M_{23} = \int_{Area} \sigma(L_1) \lambda L_1 darea \tag{10}$$

where λ is the height of the triangle 123, Fig. 6. Performing the integration it becomes

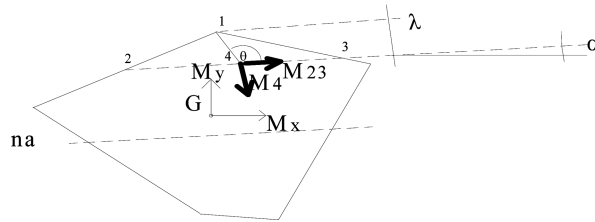


Fig. 6 Bending moments at point 4

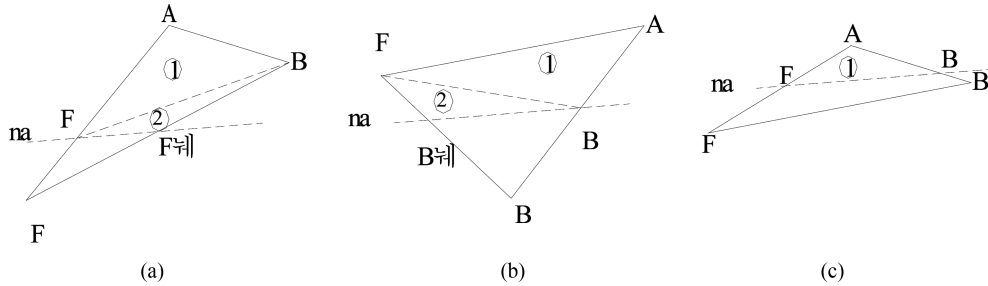


Fig. 7 (a), (b) and (c) Triangles intersected by the neutral axis

$$M_{23} = \int_0^1 \sigma(L_1) \lambda L_1 (1-L_1) \det J \, dL_1 \tag{11}$$

Considering that point 4 is located at the middle of segment 23 and denoting by θ the angle between this segment and direction 41, see Fig. 6, the bending moment M_4 , in the direction normal to 23, is given by

$$M_4 = M_{23} / \tan \theta \tag{12}$$

2.3 Tensile zone

If the neutral axis intersects the section, the triangles in the tensile zone are not considered in the summation of force and bending moments, since tension in concrete is not considered in the ultimate design. If a triangle is intersected by the neutral axis, there are different possibilities to be studied, as represented in Fig. 7. In Figs. 7(a) and (b) a subdivision into triangles 1 and 2 is considered and in Fig. 7(c) only triangle 1 is necessary. The integration process is performed for the new triangles as described previously.

2.4 Bending moments at the centroid of the section

The bending moments at the centroid of the section and directions x and y , termed M_x and M_y , are obtained by the following transformations, according to Fig. 6

$$M_x = M_{23} \cos \alpha + M_4 \sin \alpha + Fy_4 \tag{13}$$

$$M_y = M_{23} \sin \alpha - M_4 \cos \alpha - Fx_4 \tag{14}$$

where x_4 and y_4 are the coordinates of point 4.

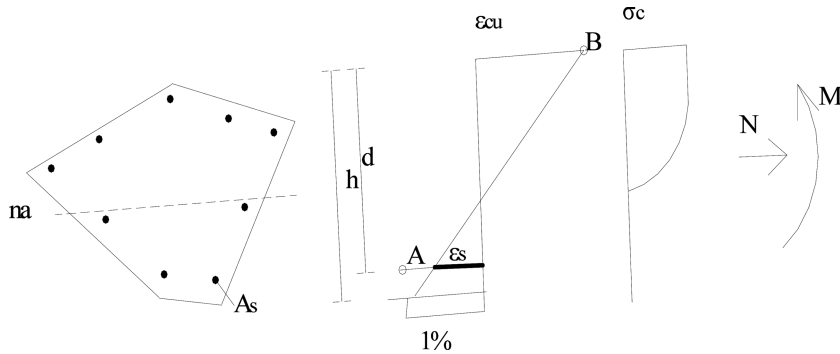


Fig. 8 Deformed section and corresponding concrete stresses

3. Service stresses

To evaluate the conditions of the reinforced concrete under service load it is necessary to obtain the stresses due to imposed bending moment M and axial load N . For this purpose the neutral axis position (na), defined by n and angle β in Eq. (1), must be known as well as the maximum concrete strain ε_c , as shown in Fig. 8.

This is a difficult task due to the fact that concrete stresses are described by nonlinear equations that are integrated over a variable domain because of the change of the neutral axis. In the present work the mathematical manipulation program is solved for the inverse problem. The bending moment M and axial load N are obtained for given positions of neutral axis, defined by the non dimensional parameter $\alpha = X/d$ (since X is easily related to n and $\beta = 0$) and increasing strain ε_c varying within the range of 0 up to the ultimate value, that is $0 \leq \varepsilon_c \leq \varepsilon_{cu}$, as shown in Fig. 8. This procedure ends at the ultimate section design load, that corresponds to the rupture values M_{rd} and N_{rd} .

4. Algorithm of solution

The algorithm of solutions consists of the following steps:

- (1) Geometry definition
 - Read the number of points defining the shape of the section
 - Read the coordinates of the contour points
- (2) For an arbitrary neutral axis defined by Eq. (1)
 - Define the deformation with Eq. (3)
 - Evaluate the distance of contour points to the neutral axis
 - Evaluate the maximum and minimum distance of contour points
 - Decompose the section in triangles
- (3) For each triangle i
 - Evaluate the integral Eq. (9), defining F_i
 - Evaluate moments M_{xi} and M_{yi} by Eqs. (13) and (14)
- (4) Accumulate the contributions of each triangle

$$F = \sum F_i \quad M_x = \sum M_{xi} \quad M_y = \sum M_{yi}$$

5. Numerical results

As mentioned before the model permits any type of constitutive Eq. (7) in defining concrete stresses. The work developed here uses the parabola-rectangle law of EC2 that, using Heaviside functions, becomes

$$\sigma(L_1) = \left(-f_{cd} \left(1 - \left(1 + \frac{\varepsilon_c L_1}{\varepsilon_{c2}} \right)^\kappa \right) H(\varepsilon_{c2} + \varepsilon_c L_1) \right) - f_{cd} H(-\varepsilon_{c2} - \varepsilon_c L_1) \tag{15}$$

The parameters used in the examples are $\kappa=2$, $\varepsilon_{c2} = 0.002$ and $\varepsilon_{cu} = -0.0035$.

5.1 Square section

The model is used in the evaluation of resulting force and bending moment in the square concrete section of Fig. 9(a) with sides $2\text{ m} \times 2\text{ m}$. The parameters for the definition of the concrete stress are $n=2$, $f_{cd} = 25.0\text{ MPa}$, $\varepsilon_{cu} = -0.0035$ and $\varepsilon_{c2} = 0.002$.

In Figs. 9-12(a) are represented the section and different positions of the neutral axis. Figs. 9-12(b) represent the corresponding stress diagram in the compressed concrete.

Table 1 summarizes the force and bending moments obtained with the model and the analytical results for the case of Fig. 10. These results are coincident up to eight digits.

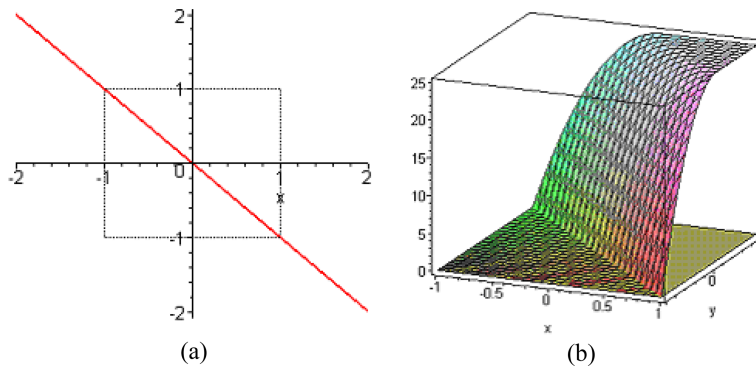


Fig. 9 (a) Square section and neutral axis position $\alpha = -\pi/4$ and $n = 0$ and (b) Corresponding stresses

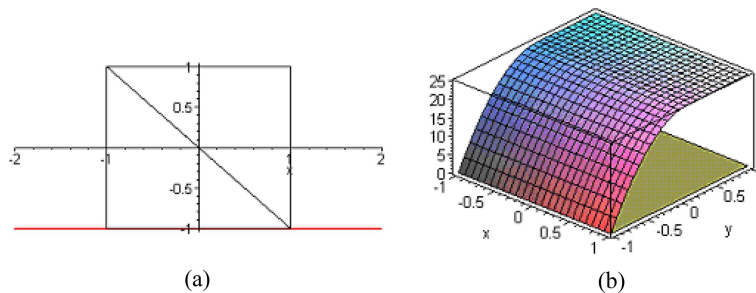


Fig. 10 (a) Neutral axis position $\alpha = 0$ and $n = -1$ and (b) Corresponding stresses

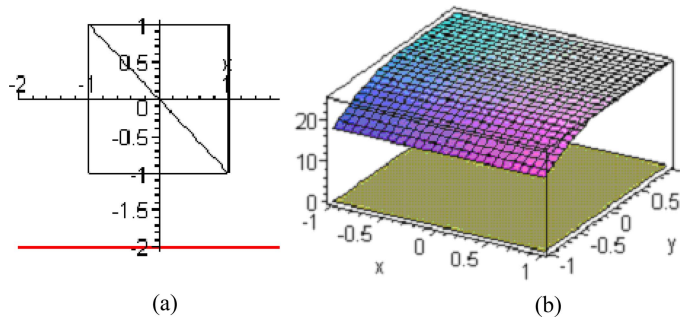


Fig. 11 (a) Neutral axis position $\alpha = 0$ and $n = -2$ and (b) Corresponding stresses

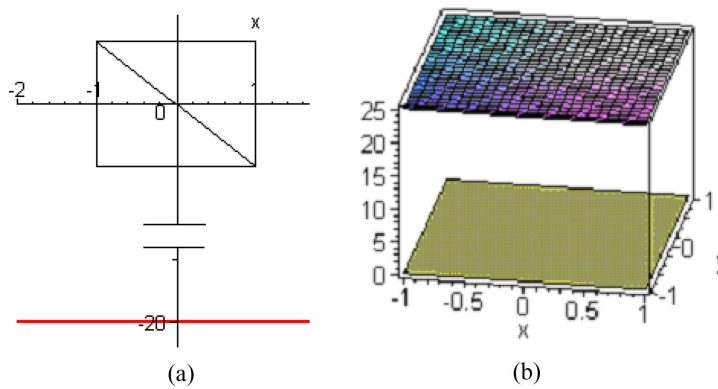


Fig. 12 (a) Neutral axis position $\alpha = 0$ and $n = -20$ and (b) Corresponding stresses

Table 1 Resulting force and bending moments

α	n (m)	F (MN)	M_x (MNm)	M_y (MNm)
$\alpha = -\pi/4$ Fig. 9	$n = 0$	-33.67346938	-14.56754129	-14.56754129
$\alpha = 0$ Fig. 10	$n = -1$	-80.952381	-13.605442	0.1 10 ⁻⁷
	Analytical	-80.952381	-13.605442	0
$\alpha = 0$ Fig. 11	$n = -2$	-94.58201068	-3.86999243	0
$\alpha = 0$ Fig. 12	$n = -20$	-99.93868271	-0.04379806	-0.1 10 ⁻⁷
$\alpha = 0$	$n = -100$	-99.99751959	-0.00177214	0
$\alpha = 0$	$n = \infty$	-100	0	0

5.2 Irregular section

We consider now the irregular section represented in Fig. 13(a), in which the dimensions are defined in meters. The section is divided into the triangles indicated and the stresses are represented in Fig. 13(b). The resulting force is $F = -105.9676901$ MN and bending moments $M_x = 107.8344365$ MNm and $M_y = 408.8386702$ MNm.

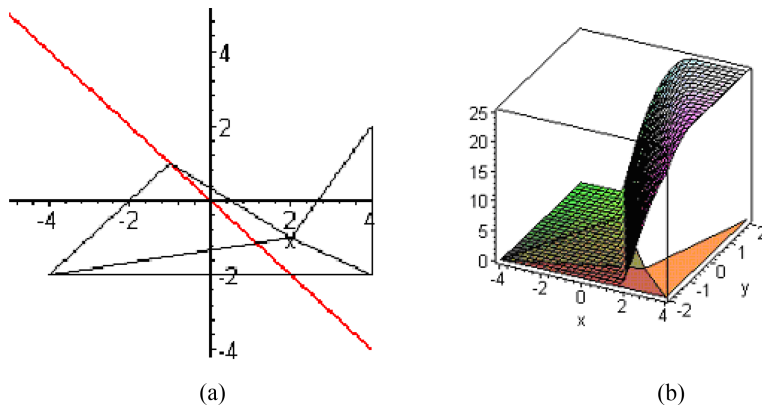


Fig. 13 (a) Neutral axis position $\alpha = -\pi/4$ and $n = 0$ and (b) Corresponding stresses

5.3 Section in L shape

The section in L shape represented in Fig. 14(a) is also analysed using the same type of concrete. Figs. 14 and 15(a) show the neutral axis position and Figs. 14 and 15(b) show the stresses in the section.

In Table 2 are summarized the results for this section showing a coincidence of eight digits for the

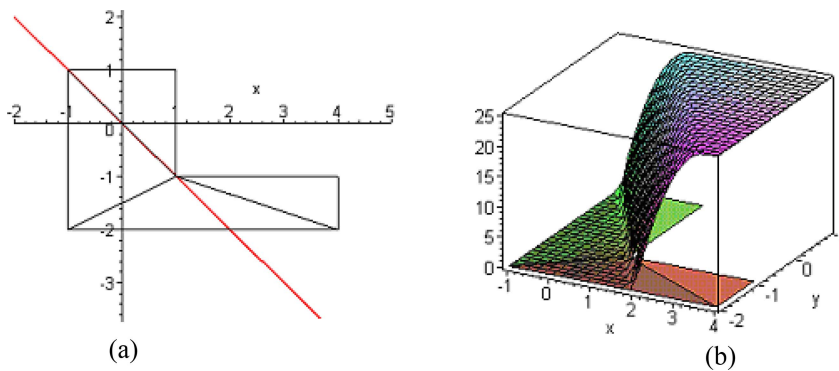


Fig. 14 (a) Neutral axis position $\alpha = -\pi/4$ and $n = 0$ and (b) Corresponding stresses

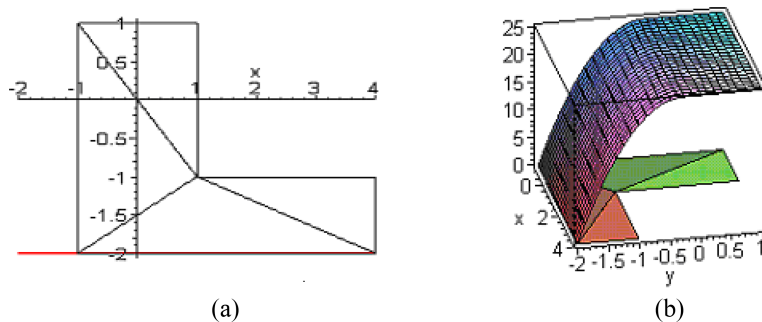


Fig. 15 (a) Neutral axis position $\alpha = 0$ and $n = -2$ and (b) Corresponding stresses

Table 2 Resulting force and bending moments in L section

α	n (m)	F (MN)	M_x (MNm)	M_y (MNm)
$\alpha = -\pi/4$ Fig. 14	$n = 0$	-75.76530615	57.59475220	155.925650
$\alpha = 0$ Fig. 15	$n = -2$	-156.67163	77.80169	88.10764
	Analytical	-156.67163	77.80169	88.10764

force and seven for the bending moment.

5.4 Abacus for service stresses in rectangular section

The algorithm is applied to a rectangular reinforced concrete section with reinforcement ratio $w = (A + A') / (bh f_{cd}) = 0.1$ and $A' / A = 1.0$. Reduced axial load is $\nu = N / (bh f_{cd})$ and reduced bending moment is $\mu = M / (bh^2 f_{cd})$. The maximum stress in concrete is $\alpha' f_{cd} = 1.0 f_{cd}$.

In Fig. 16 can be observed that strain ϵ_c increases progressively until it reaches the ultimate

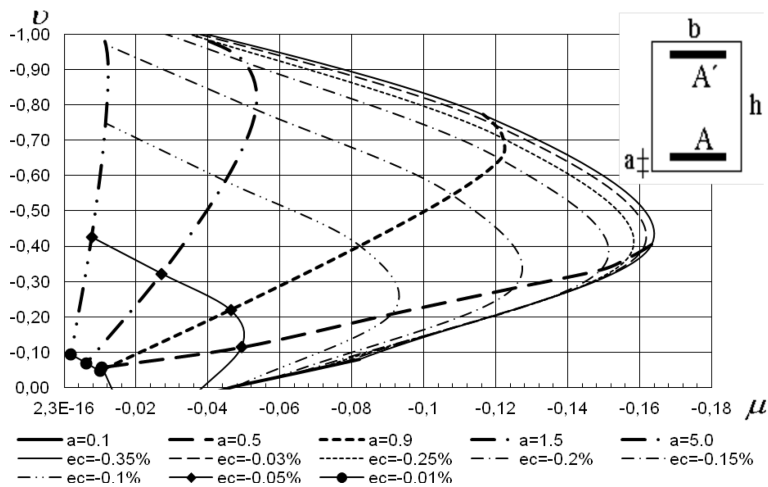


Fig. 16 Interaction diagram for constant values α and increasing ϵ_c , with $A' / A = 1.0$ and $w = 0.1$

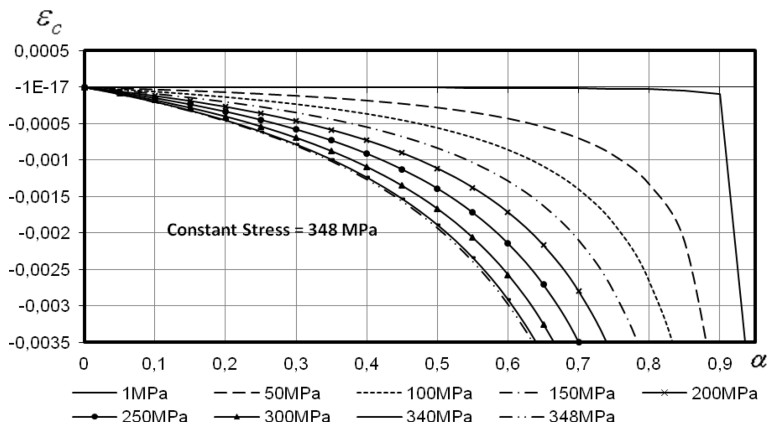


Fig. 17 Stress σ_s at reinforcing steel A obtained for variable ϵ_c and α

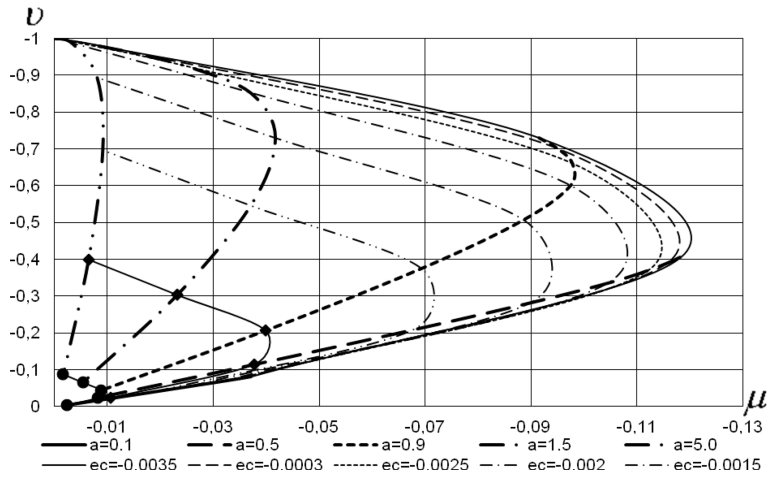


Fig. 18 Interaction diagram for constant values α and increasing ε_c for the section without reinforcing steel

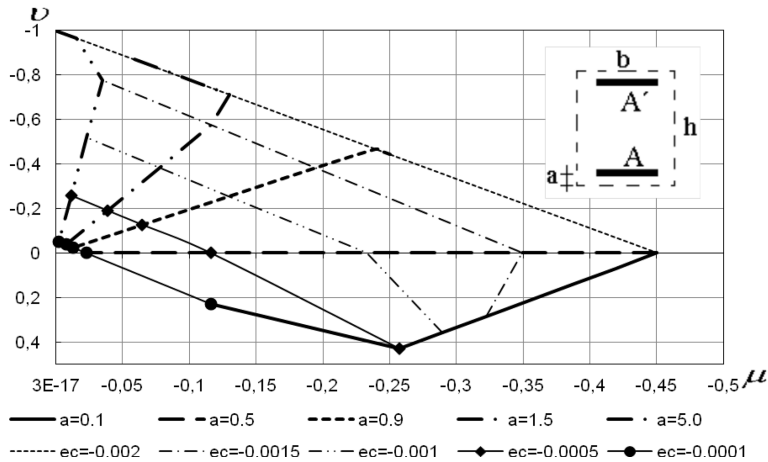


Fig. 19 Interaction diagram for constant values α and increasing ε_c for the section with reinforcing steel $A'/A = 1.0$ and $w = 1.0$

interaction diagram that is the contour diagram for the indicated section.

Fig. 17 represents the stress σ_s at steel A obtained as a function of ε_c and α , obtained from Fig. 16. The formula for σ_s is summarized in Appendix A. To evaluate the stress in the steel for given values of M_1 and N_1 , the reduced bending moment μ_1 and axial load ν_1 are calculated. Then Fig. 16 is used to find the corresponding $(\varepsilon_c)_1$ and α_1 by interpolation; the abacus of Fig. 17 gives the stress in the steel A .

The abacus in Fig. 16 can be obtained from the interaction diagram for concrete in Fig. 18 added to the abacus in Fig. 19 multiplied by $w = 0.1$, since this figure is made for $w = 1.0$.

Other abacuses can be obtained, for instance Fig. 20 represents the abacus for $A'/A = 0.5$ and $w = 1.0$. Multiplied by the w of the section and adding it to the interaction diagram for concrete in Fig. 18, different design abacus for reinforcement ratio $A'/A = 0.5$ can be constructed.

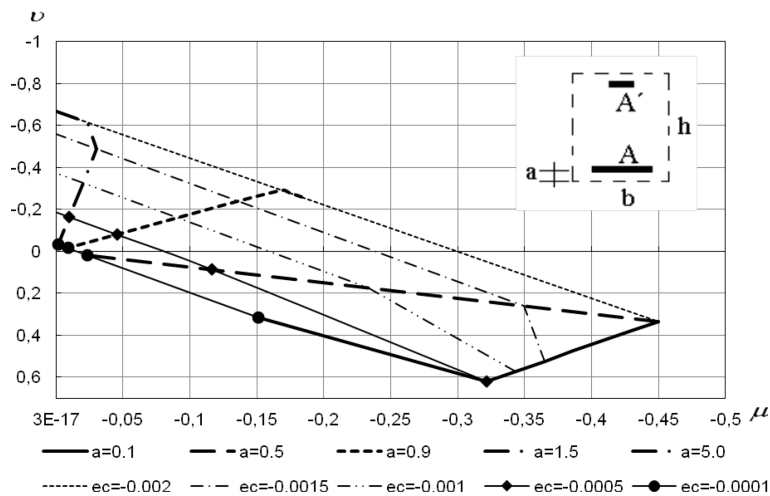


Fig. 20 Interaction diagram for constant values α and increasing ε_c for the section with reinforcing steel $A'/A = 0.5$ and $w = 1.0$

6. Conclusions

A model for the integration of concrete stresses in a section under axial force and biaxial bending moment is presented. The model can be used in any section described by a closed polygonal line. The model is implemented into a mathematical manipulation program and the results obtained are coincident to the theoretical values up to the desired number of digits.

With this model design abacus for ultimate as well as service stresses in different reinforced concrete sections can be obtained. It is our intention to extend this work to sections with curved boundaries, in particular circular sections.

Acknowledgments

The support from Laboratory for the Concrete Technology and Structural Behaviour – LABEST, Faculty of Engineering of the University of Porto (FEUP) is acknowledged.

References

- Alnuaimi, A.S. (2007), "Direct design of partially prestressed concrete solid beams", *Struct. Eng. Mech.*, **27**(6), 741-771.
- Barros, M.H.F., Barros, A.F.M. and Ferreira, C.C. (2004), "Closed form solution of optimal design of rectangular reinforced concrete sections", *Eng. Computat.*, **21**(7), 761-776.
- Barros, M.H.F.M. and Martins, R.A.F (2006), "Nonlinear analysis of service stresses in reinforced concrete sections using closed form solutions", *5th Int. Conf. on Mechanics and Materials in Design*, M2D.
- Barros, M.H.F.M., Ferreira, C.C. and Barros, A.F.M. (2003), "Integração do diagrama de tensões de compressão do betão em flexão desviada usando a equação do MC90", *Construlink*, www.construlink.com, **1**(3), 41-49.

- Barros, M.H.F.M., Ferreira, C.C. and Barros, A.F.M. (2005), "Closed form interaction surfaces for nonlinear design codes of reinforced concrete columns with model code 90", *Comput. Concrete*, **2**(1), 55-77.
- Bonet, J.L., Barros, M.H.F.M. and Romero, M.L. (2006), "Comparative study of analytical and numerical algorithms for design reinforced concrete sections under biaxial bending", *Comput. Struct.*, **84**(31-32), 2184-2193.
- Campion, G (2008), "Analytical model for high-strength concrete columns with square cross-section", *Struct. Eng. Mech.*, **28**(3), 295-316.
- CEB-FIP Model Code 1990 (1991), *Committee Euro-International du Beton*, CEB Bulletin n°203-204 e 205 Thomas Telford.
- Charalampakis, A.E. and Koumousis, V.K. (2008), "Ultimate strength analysis of composite sections under biaxial bending and axial load", *Adv. Eng. Softw.*, **39**(11), 923-936.
- Chaudhary, S., Pendharkar, U. and Nagpal, A.K. (2007), "An analytical-numerical procedure for cracking and time-dependent effects in continuous composite beams under service load", *Steel Compos. Struct.*, **7**(3), 219-240.
- EC2 Eurocode 2 (2003), *Design of concrete structures*, PrEN 1992-1-1, European Committee for Standardization.
- Fragiadakis, M. and Papadrakakis, M. (2008), "Performance-based optimum seismic design of reinforced concrete structures", *Earthq. Eng. Struct. D.*, **37**(6), 825-844.
- Lam, J.Y.K., Ho, J.C.M. and Kwan, A.K.H. (2009), "Maximum axial load level and minimum confinement for limited ductility design of high-strength concrete columns", *Comput. Concrete*, **6**(5), 357-376.
- Lou, T.J. and Xiang, Y.Q. (2008), "Numerical method for biaxially loaded reinforced and prestressed concrete slender columns with arbitrary section", *Struct. Eng. Mech.*, **28**(5), 587-601.
- Pallares, L., Miguel, P.F. and Fernandez-Prada, M.A. (2009), "A numerical method to design reinforced concrete sections subjected to axial forces and biaxial bending based on ultimate strain limits", *Eng. Struct.*, **31**(12), 3065-3071.
- Papadakis, V.G., Efstathiou, M.P. and Apostolopoulos, C.A. (2007), "Computer-aided approach of parameters influencing concrete service life and field validation", *Comput. Concrete*, **4**(1), 1-18.
- Rami, A. Hawileh, Faris, A. Malhas and Rahman, A. (2009), "Comparison between ACI 318-05 and Eurocode 2(EN1992-1-1) in flexural concrete design", *Struct. Eng. Mech.*, **32**(6), 705-724.
- Ruiz, M.F., Muttoni, A. and Gambarova, P.G. (2007), "Analytical modeling of the pre- and postyield Behavior of bond in reinforced concrete", *J. Struct. Eng.-ASCE*, **133**(10), 1364-1372.
- Sadjadi, R. and Kianoush, M.R. (2010), "Application of fiber element in the assessment of the cyclic loading behavior of RC columns", *Struct. Eng. Mech.*, **34**(3), 301-317.
- Silva, V. Dias, Barros, M.H.F.M., Julio, E.N.B.S. and Ferreira, C.C. (2009), "Closed form ultimate strength of multi-rectangle reinforced concrete sections under axial load and biaxial bending", *Comput. Concrete*, **6**(6), 505-521.
- Sousa, J.B.M. and Muniz, C.F.D.G. (2007), "Analytical integration of cross section properties for numerical analysis of reinforced concrete, steel and composite frames", *Eng. Struct.*, **29**(4), 618-625.

Appendix A.

The formula for F and σ_s are the following

$$\begin{aligned}
 F = & -\left(-f_{cd}\left(\frac{(e_{c2}+e_2)^4}{4(e_1-e_2)^2 e_{c2}^2} - \frac{\left(1\left(1+\frac{e_2}{e_{c2}}\right)(e_1-e_2) - \frac{(e_1-e_2)^2}{e_{c2}^2}\right)(e_{c2}+e_2)^3}{3(e_1-e_2)^2}\right)\right. \\
 & + \frac{\left(-1+\left(1+\frac{e_2}{e_{c2}}\right)^2\right) - \frac{2\left(1+\frac{e_2}{e_{c2}}\right)(e_1-e_2)}{e_{c2}}(e_{c2}+e_2)^2}{2(e_1-e_2)^2} - \frac{e_{c2}+e_2}{e_1-e_2} + \frac{\left(1+\frac{e_2}{e_{c2}}\right)^2(e_2+e_2)}{e_1-e_2})\text{Heaviside}(e_{c2}+e_2) \\
 & + \left(-f_{cd}\left(-\frac{(e_1-e_2)^2}{12e_{c2}^2} - \frac{\left(1+\frac{e_2}{e_{c2}}\right)(e_1-e_2)}{3e_{c2}} + \frac{1}{2} - \frac{\left(1+\frac{e_2}{e_{c2}}\right)^2}{2}\right) + f_{cd}\left(\frac{(e_{c2}+e_2)^4}{4(e_1-e_2)^2 e_{c2}^2}\right.\right. \\
 & \left.\left. - \frac{\left(2\left(1+\frac{e_2}{e_{c2}}\right)(e_1-e_2) - \frac{(e_1-e_2)^2}{e_{c2}^2}(e_{c2}+e_2)^3\right)}{3(e_1-e_2)^3} + \frac{\left(-1+\left(1+\frac{e_2}{e_{c2}}\right)^2 - \frac{2\left(1+\frac{e_2}{e_{c2}}\right)(e_1-e_2)}{e_{c2}}\right)(e_{c2}+e_2)^2}{2(e_1-e_2)^2} - \frac{e_{c2}+e_2}{e_1-e_2}\right.\right. \\
 & \left.\left. + \frac{\left(1+\frac{e_2}{e_{c2}}\right)^2(e_{c2}+e_2)}{e_1-e_2}\right)\right)\text{Heaviside}(e_{c2}+e_1) - f_{cd}\left(-\frac{(e_{c2}+e_2)^2}{2(e_1-e_2)^2} - \frac{e_{c2}+e_2}{e_1-e_2}\right)\text{Heaviside}(-e_{c2}-e_2) \\
 & + \left(\frac{f_{cd}}{2} + f_{cd}\left(-\frac{(e_{c2}+e_2)^2}{2(e_1-e_2)^2} - \frac{e_{c2}+e_2}{e_1-e_2}\right)\right)\text{Heaviside}(-e_{c2}-e_1))(y_A y_F x_A + y_B y_F x_A + 2y_B y_A x_F - x_B y_B y_A) \\
 & + x_B y_B y_F - y_B x_A y_A - y_A x_B y_F + y_B^2 x_A - y_B^2 x_F + y_A^2 x_B - y_A^2 x_F) / (-y_A + y_F) \\
 \sigma_s = & f_{syd} \text{Heaviside}\left(\frac{e_c\left(\frac{h-a}{h}-\alpha\right) - \frac{f_{syd}}{E_s}}{\alpha}\right) - \frac{e_c\left(\frac{h-a}{h}-\alpha\right) E_s \text{Heaviside}\left(\frac{e_c\left(\frac{h-a}{h}-\alpha\right)}{\alpha} + \frac{f_{syd}}{E_s}\right)}{\alpha} \\
 & + \frac{e_c\left(\frac{h-a}{h}-\alpha\right) E_s \text{Heaviside}\left(\frac{e_c\left(\frac{h-a}{h}-\alpha\right)}{\alpha} - \frac{f_{syd}}{E_s}\right)}{\alpha} - f_{syd} \text{Heaviside}\left(\frac{e_c\left(\frac{h-a}{h}-\alpha\right)}{\alpha} - \frac{f_{syd}}{E_s}\right)
 \end{aligned}$$